

Light-Induced N₂O Production from a Non-heme Iron–Nitrosyl Dimer

Yunbo Jiang,[†] Takahiro Hayashi,^{†,§} Hirotoshi Matsumura,[†] Loi H. Do,^{‡,⊥} Amit Majumdar,^{‡,||} Stephen J. Lippard,^{*,‡} and Pierre Moënne-Loccoz^{*,†}

[†]Institute of Environmental Health, Oregon Health and Science University, Portland, Oregon 97239, United States

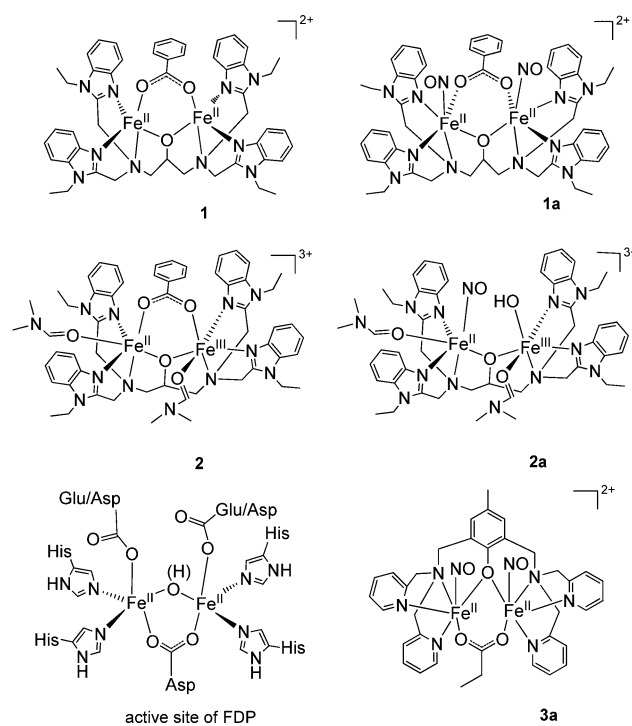
[‡]Department of Chemistry, Massachusetts Institute of Technology, Cambridge, Massachusetts 02139, United States

Supporting Information

ABSTRACT: Two non-heme iron–nitrosyl species, [Fe₂(N-Et-HPTB)(O₂CPh)(NO)₂](BF₄)₂ (**1a**) and [Fe₂(N-Et-HPTB)(DMF)₂(NO)(OH)](BF₄)₃ (**2a**), are characterized by FTIR and resonance Raman spectroscopy. Binding of NO is reversible in both complexes, which are prone to NO photolysis under visible light illumination. Photoproduction of N₂O occurs in high yield for **1a** but not **2a**. Low-temperature FTIR photolysis experiments with **1a** in acetonitrile do not reveal any intermediate species, but in THF at room temperature, a new {FeNO}⁷ species quickly forms under illumination and exhibits a ν(NO) vibration indicative of nitroxyl-like character. This metastable species reacts further under illumination to produce N₂O. A reaction mechanism is proposed, and implications for NO reduction in flavodiiron proteins are discussed.

Nitric oxide (NO) plays an important role in cellular signaling in a wide range of biological processes. NO can also be toxic when present at high concentration, and it participates as a key immune defense agent against invading pathogens. Accordingly, a variety of detoxifying enzymes have evolved in pathogens, and understanding their microbial NO defense mechanisms may provide new strategies for controlling infections.^{1–7} In anaerobic environments, NO detoxification occurs via the two-electron reduction of NO to form nitrous oxide (N₂O). Flavodiiron proteins (FDPs) are flavin-containing, NO-detoxifying enzymes with an active site containing a non-heme diiron cluster (see Chart 1).⁴ In most FDPs,⁸ each metal ion is coordinated by two His ligands and one terminal monodentate carboxylate group from either Asp or Glu; a bridging bidentate Asp and a water-derived ligand (oxo or hydroxo) complete the coordination sphere. An open coordination site remains on each Fe(II). Both mono- ({FeNO}⁷) and dinitrosyl ([{FeNO}⁷]₂) FDP adducts have been characterized.^{9,10} Experiments with a flavin-free form of the enzyme reveal that N₂O production can occur without the flavin mononucleotide (FMN) cofactor.¹⁰ An exceptionally low frequency ν(NO) band at 1681 cm⁻¹ was detected in mononitrosyl complexes of FMN-free and FMN-containing enzymes, which suggests a nitroxyl-like configuration of the {FeNO}⁷ unit.⁹ Electrostatic interaction of this nitroxyl-like group with the adjacent Fe^{II} center could prime the mononitrosyl complex for electrophilic attack by a second NO.⁹ In contrast, the [{FeNO}⁷]₂ adduct persists in the FMN-free enzyme, suggesting that it either

Chart 1. Structural Comparison of Complexes **1**, **1a**, **2**, **2a**, **3a**, and the Active Site of FDP



corresponds to an inactive state¹⁰ or may be poised for reduction by FMN in the flavinated enzyme.⁴

Non-heme iron synthetic models provide insight into the catalytic mechanism of FDP proteins. The first report of a non-heme diiron–dinitrosyl compound, [Fe₂(N-Et-HPTB)(O₂CPh)(NO)₂](BF₄)₂ (**1a**, N-Et-HPTB = N,N,N',N'-tetrakis(2-(1-ethylbenzimidazolyl))-2-hydroxy-1,3-diaminopropane), detailed a full characterization of the model complex by single-crystal X-ray diffraction, UV/vis, IR, and Mössbauer spectroscopy, and magnetic susceptibility measurements. It also revealed **1a** to be stable in an acetonitrile solution for over a day at room temperature.¹¹ A mixed-valent diiron–mononitrosyl complex, [Fe₂(N-Et-HPTB)(OH)(NO)(DMF)₂](BF₄)₃ (**2a**), with the N-Et-HPTB ligand was also isolated.¹² Recently, an iron–nitrosyl dimer, [Fe₂(BPMP)(OPr)(NO)₂](BPh₄)₂ (**3a**, BPMP = 2,6-bis[bis(2-pyridylmethyl)amino]methyl)-4-methyl-

Received: May 6, 2014

Published: August 12, 2014

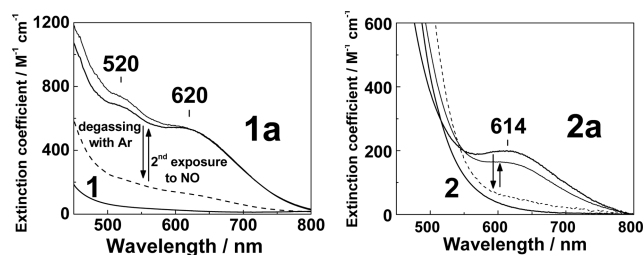


Figure 1. Electronic spectra of **1** and **1a** (left panel) and **2** and **2a** (right panel) in acetonitrile at room temperature. Also shown are the effects of purging solutions of **1a** and **2a** with Ar for 3 min (dashed lines) before repeated exposure to NO.

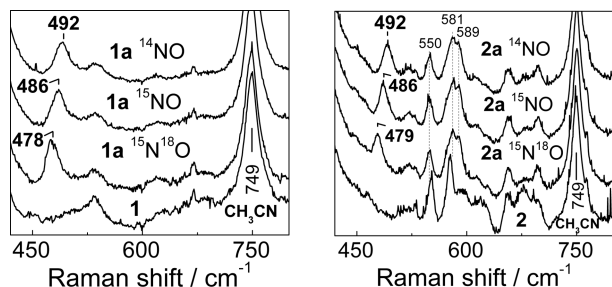


Figure 2. Resonance Raman spectra of **1** and **1a** (left panel) and **2** and **2a** (right panel) at room temperature ($\lambda_{\text{exc}} = 458 \text{ nm}$, $[\mathbf{1}]$, $[\mathbf{1a}] = 2 \text{ mM}$, $[\mathbf{2}]$, $[\mathbf{2a}] = 2.5 \text{ mM}$).

phenolate), was structurally characterized and shown to produce N_2O upon either chemical or electrochemical reduction.¹³ This latter example supports the notion that FMN could reduce the $[\{\text{FeNO}\}^7]_2$ complex in FDP and thus allow catalytic turnover without redox cycling of the Fe(II) centers. Nevertheless, activating the $\{\text{FeNO}\}^7$ unit for attack by a second NO to produce a transient hyponitrite remains a valid alternative for the reduction of NO to N_2O .

Here we report that production of N_2O by **1a** can proceed under illumination with white light at room temperature and at 15 K. We also show that this process is preceded by simple photodissociation of NO from the iron–nitrosyl dimer. In the case of **2a**, photodissociation also occurs, but the resulting NO does not react further.

The chromophoric $\{\text{FeNO}\}^7$ units in **1a** and **2a** display distinctive nitrosyl-to-iron ligand-to-metal charge-transfer absorption bands, and these NO adducts in acetonitrile solutions easily revert to diiron(II) compounds after the sample is purged with Ar (Figure 1). The resonance Raman (RR) spectrum of **1a** obtained with 458 nm laser excitation shows a $\nu(\text{FeNO})$ band at 492 cm^{-1} with unlabeled NO that shifts to 486 cm^{-1} with ^{15}NO and to 478 cm^{-1} with $^{15}\text{N}^{18}\text{O}$ (Figure 2). Nearly identical $\nu(\text{FeNO})$ frequencies are observed in the RR spectrum of **2a**, which is consistent with the structural similarity of these $[\text{FeNO}]$ units observed by crystallography.^{11,12} Additional vibrations in the low-frequency region of the RR spectrum of **2a** cannot be assigned with certainty at this time, but these modes do not shift with NO labeling or with the addition of 20% D_2O to the acetonitrile solutions and are therefore unrelated to the nitrosyl or hydroxy ligands.

Room-temperature FTIR spectra of **1a** and **2a** in acetonitrile show $\nu(\text{NO})$ modes at 1784 and 1810 cm^{-1} , respectively, with the expected down-shifts with ^{15}NO and $^{15}\text{N}^{18}\text{O}$ (Figure 3). These $\nu(\text{NO})$ values are consistent with earlier reports^{11,12} and with the $S = 3/2$ $\{\text{FeNO}\}^7$ description of non-heme $[\text{FeNO}]$

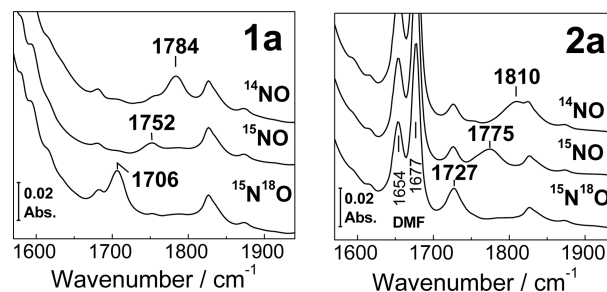


Figure 3. Room-temperature FTIR spectra of **1a** (left panel) and **2a** (right panel) at room temperature ($[\mathbf{1a}] = 18 \text{ mM}$, $[\mathbf{2a}] = 20 \text{ mM}$).

units.¹⁴ As reported previously, **1a** is composed of two $\{\text{FeNO}\}^7$ units, which have identical coordination environments and exhibit the same set of vibrational frequencies. The $\nu(\text{NO})$ band in **2a** is up-shifted by 26 cm^{-1} relative to that in **1a** and is significantly broadened, presumably because of the heterogeneity in the binding geometry and environment of the nitrosyl group in **2a**. The up-shift of the $\nu(\text{NO})$ may result from substitution of the bridging benzoate in **1a** by two DMF ligands in **2a**. Amide-like vibrations from DMF are observed for **2a** at 1654 and 1677 cm^{-1} . The latter frequency matches that of free DMF in acetonitrile, whereas the lower frequency at 1654 cm^{-1} is consistent with a lengthening of the $\text{C}=\text{O}$ bond upon coordination of DMF to metal ions.

Low-temperature FTIR spectra of **1a** reproduce the $\nu(\text{NO})$ values observed at room temperature, but those of **2a** display a significant decrease in the intensity of the $\nu(\text{NO})$ modes that is indicative of a diminished NO binding affinity at cryogenic temperatures (Figure S1). Previous differential FTIR photolysis experiments indicate that, at least within the active sites of metalloproteins, non-heme iron–nitrosyl complexes can be trapped as photodissociated states following illumination with white light at cryogenic temperatures.^{9,10,15,16} Based on these findings, “dark” minus “illuminated” FTIR difference spectra can be used to isolate $\nu(\text{NO})$ bands emanating from $\{\text{FeNO}\}^7$ species as positive features in the 1700 cm^{-1} region, whereas the photolyzed NO group is detected as a weak negative band near 1870 cm^{-1} . Typically, the buildup of the photolyzed population occurs during the first few minutes of white-light illumination, and further illumination does not produce any additional spectral changes. Geminate rebinding of the photolyzed ligand requires a slight increase in sample temperature (to $\sim 40\text{--}80 \text{ K}$), and repeating the photolysis procedure at 15 K confirms the complete reversibility of these processes. Reversible photorelease of NO from a non-heme $\{\text{FeNO}\}^7$ synthetic complex at room temperature was also reported recently.¹⁷

Low-temperature FTIR photolysis experiments with **2a** reproduce the behavior displayed previously by non-heme protein NO adducts (Figure 4). Specifically, the spectra show that the $\{\text{FeNO}\}^7$ species in **2a** is photolabile and that further illumination does not produce any additional changes. In contrast, **1a** reveals unique photoreactivity. The light-induced FTIR difference spectrum of **1a** at 15 K exhibits a positive band at 1787 cm^{-1} and a weak negative band at 1867 cm^{-1} which, based on ^{15}NO -isotope shifts, are assigned to the $\nu(\text{NO})$ of $\{\text{FeNO}\}^7$ and free NO, respectively (Figure 4). Further illumination at 15 K produces additional spectral changes, including the appearance of a negative signal at 2239 cm^{-1} that shifts to 2168 and 2162 cm^{-1} with ^{15}NO and $^{15}\text{N}^{18}\text{O}$, respectively. (Figures 4 and S2). The 2239 cm^{-1} signal and its accompanying isotope shifts are characteristic of the $\nu(\text{NN})$ mode of N_2O . This process is

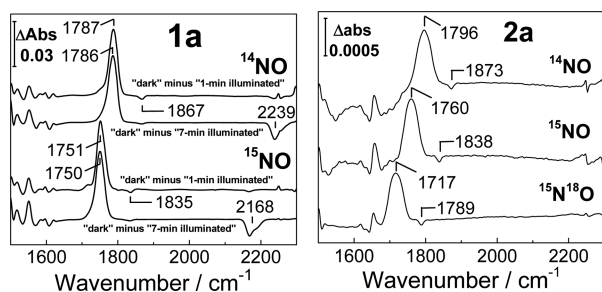


Figure 4. Light-induced FTIR difference spectra of **1a** (left panel, difference spectra for 1 and 7 min illuminations) and **2a** (right panel, difference spectra after completion of the photoprocess) at 15 K ($[1a] = 18$ mM, $[2a] = 20$ mM).

irreversible and can result in the complete consumption of **1a** after prolonged illumination at 15 K (Figure S3). FTIR samples prepared by exposing **1** to substoichiometric levels of NO produce light-induced difference spectra equivalent to those obtained with **1a**, indicating that two NO molecules bind in a cooperative fashion to **1** without significant buildup of a mononitrosyl species (Figure S4). Comparing the integration of the $\nu(\text{NN})$ signal generated from **1a** after illumination at 15 K with titration curves generated using N_2O -saturated acetonitrile suggests that the formation of N_2O proceeds with a high yield ($\sim 90\%$ at 15 K, Figure S5). These FTIR experiments indicate that white-light illumination of **1a** initially produces a population of caged-in dissociated NO that can react with the diiron complex to subsequently generate N_2O under further illumination. Because this reaction occurs at 15 K, an intermolecular process between two or more **1a** diiron complexes can be ruled out. In addition, decreasing the concentration of **1a** does not significantly affect the illumination time required for the formation of N_2O (data not shown).

Because the reduction of two NO molecules to N_2O requires two electrons, the other product of the photoreaction is likely to be a diiron(III) complex. EPR spectra of **1a** obtained after illumination at 15 K showed no signal that could be assigned as Fe(III) centers (data not shown), suggesting antiferromagnetic coupling between the two Fe(III) centers. RR spectroscopy was used to determine whether a (μ -oxo)diiron(III) product is formed after the release of N_2O , but the results were inconclusive.

Production of N_2O from **1a** under illumination is also observed at room temperature in acetonitrile and THF, although with reduced yields compared to those at low temperature (15% and 26%, respectively). FTIR spectra of **1a** in THF collected in the dark and after consecutive 1 min illuminations reveal a loss of the $\nu(\text{NO})$ at 1781 cm^{-1} in favor of a signal at 1695 cm^{-1} that shifts to 1665 cm^{-1} with ^{15}NO , and a minor intensity gain in the $\nu(\text{NN})$ of N_2O at 2223 cm^{-1} (Figure 5, top traces). After the first 2 min of irradiation, subsequent illuminations lead to growth of the $\nu(\text{NN})$ signal and concurrent decreases in $\nu(\text{NO})$ and the peak at 1695 cm^{-1} (Figure 5, lower traces). Differential FTIR spectra for the initial and later phases of the photoprocess also help isolate light-induced features below 1600 cm^{-1} that are insensitive to NO-isotope substitution and are likely to reflect minor perturbations of vibrational modes from the *N*-Et-HPTB ligand and the benzoate bridge (Figure S6).

Time-dependent traces for the decay of the 1781 cm^{-1} $\nu(\text{NO})$ band from **1a** and the growth of the 2223 cm^{-1} $\nu(\text{NN})$ band from N_2O are shown in Figure 6. The intensity gain at 2223 cm^{-1} fits a single-exponential rate of 0.2 min^{-1} . The time trace for the

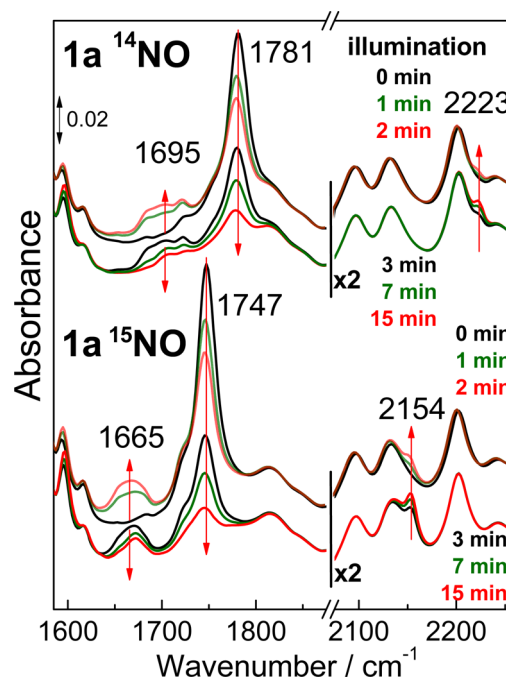


Figure 5. Room-temperature FTIR spectra of **1a** prepared in THF with ^{14}NO (top traces) or ^{15}NO (lower traces). Spectra were collected in the dark and after illumination periods of 1, 2, 3, 7, and 15 min.

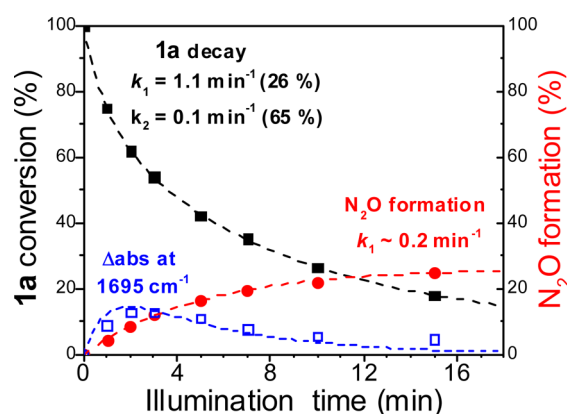
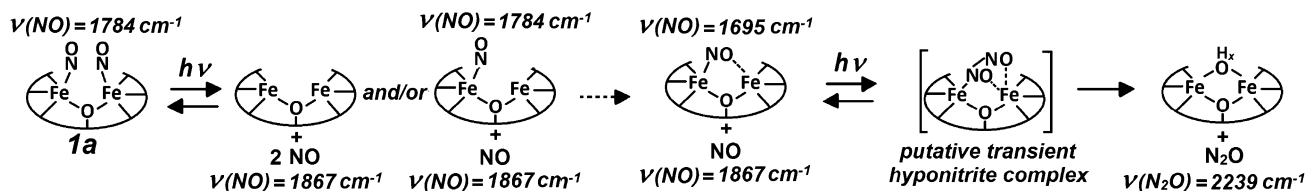


Figure 6. Progression of the FTIR intensity for $\nu(\text{NO})$ of **1a** (black squares) and $\nu(\text{NN})$ of N_2O (red circles) and for the 1695 cm^{-1} signal (open blue squares) (see Supporting Information for details).

intensity loss of the $\nu(\text{NO})$ of **1a** requires a biexponential fit with rate constants of 1.1 and 0.1 min^{-1} . The fast phase represents 26% of the overall amplitude of the signal change and matches the yield of N_2O ; presumably, the slower phase reflects side reactions that do not produce N_2O . Analyzing the time progression of the 1695 cm^{-1} signal is less reliable because of its weak intensity and because expected diiron(III) products are likely to give weak signals below 1700 cm^{-1} . Nevertheless, it is worthwhile to compare the progression of this signal by means of a simulation curve for an intermediate species with formation and decay rates that correspond to the 1.1 min^{-1} decay of **1a** and the 0.2 min^{-1} formation of N_2O (Figure 6).

The 1695 cm^{-1} FTIR signal and its 30 cm^{-1} down-shift with ^{15}NO are consistent with a $\nu(\text{NO})$ from an iron–nitrosyl complex with $[\text{Fe}^{\text{III}}-\text{NO}^-]$ nitroxyl-like character. However, this $\nu(\text{NO})$ frequency is unusually low for a non-heme $\{\text{FeNO}\}^7$ species and is reminiscent of the 1681 cm^{-1} band seen in the

Scheme 1. Possible Mechanistic Steps for the Light-Induced Production of N₂O from 1a¹⁹

FTIR spectra of the mononitrosyl adducts of the FDP from *Thermotoga maritima*, which also shows a 30 cm⁻¹ down-shift with ¹⁵NO. Such nitrosyl-like character may result from semi-bridging interactions of the NO group that render these mononitrosyl complexes susceptible to side-on electrophilic attack by a second NO to produce transient hyponitrite complexes that subsequently decay to form N₂O. Theoretical analyses of NO reduction in FDPs favor a mechanism where the formation of a partially reduced NO group in a diiron–mononitrosyl complex allows for attack by a second NO to form the N–N bond.¹⁸

From these data, we propose that the metastable nitroxyl-like mononitrosyl complex observed in THF at room temperature is a competent intermediate in the light-induced formation of N₂O via electrophilic attack by a second NO molecule (Scheme 1). Although light activation is not required for catalytic activity in FDPs, and a recent pre-steady-state study of FDP favors a diferrous–dinitrosyl intermediate as the precursor to N–N bond formation,²⁰ characterizing non-equilibrium states in synthetic models provides insight into possible reaction mechanisms and transition states that enzymes may stabilize to optimize their catalytic activity. Efforts are underway in our laboratories to further characterize this chemistry using monochromatic laser illumination as a possible way to better control the formation and decay of the 1695 cm⁻¹ species. We will also explore the possible role of protons in the reduction of NO as we did previously for the dioxygen activation reaction of these diiron models.²¹

■ ASSOCIATED CONTENT

● Supporting Information

FTIR spectra of 1a and 2a at 15 K; light-induced FTIR difference spectra of 1a prepared with NO, ¹⁵NO, and ¹⁵N¹⁸O; room-temperature UV/vis spectra of 1a before and after prolonged illumination at 15 K; 15 K FTIR spectra of N₂O in acetonitrile; room-temperature FTIR difference spectra of 1a prepared with NO and ¹⁵NO, after 2 and 15 min illumination. This material is available free of charge via Internet at <http://pubs.acs.org>.

■ AUTHOR INFORMATION

Corresponding Authors

lippard@mit.edu
moennelo@ohsu.edu

Present Addresses

[§]T.H.: Department of Synthetic Chemistry and Biological Chemistry, Graduate School of Engineering, Kyoto University
[†]L.H.D.: Department of Chemistry, University of Houston
^{||}A.M.: Department of Inorganic Chemistry, Indian Association for the Cultivation of Science

Notes

The authors declare no competing financial interest.

■ ACKNOWLEDGMENTS

This work was supported by NIH grants GM074785 (P.M.L.) and GM032134 (S.J.L.) from the National Institute of General Medical Science, the National Science Foundation (S.J.L.), a JSPS fellowship for H.M., and a Vertex pharmaceutical scholarship for T.H. We thank Mik Minier for helpful discussions.

■ REFERENCES

- (1) Gardner, A. M.; Gardner, P. R. *J. Biol. Chem.* **2002**, *277*, 8166.
- (2) Gardner, A. M.; Helmick, R. A.; Gardner, P. R. *J. Biol. Chem.* **2002**, *277*, 8172.
- (3) Gomes, C. M.; Giuffrè, A.; Forte, E.; Vicente, J. B.; Saraiva, L. M.; Brunori, M.; Teixeira, M. *J. Biol. Chem.* **2002**, *277*, 25273.
- (4) Kurtz, D. M., Jr. *Dalton Trans.* **2007**, 4115.
- (5) Le Fourn, C.; Fardeau, M.-L.; Ollivier, B.; Lojou, E.; Dolla, A. *Environ. Microbiol.* **2008**, *10*, 1877.
- (6) Saraiva, L. M.; Vicente, J. B.; Teixeira, M. *Adv. Microb. Physiol.* **2004**, *49*, 77.
- (7) Silaghi-Dumitrescu, R.; Coulter, E. D.; Das, A.; Ljungdahl, L. G.; Jameson, G. N.; Huynh, B. H.; Kurtz, D. M., Jr. *Biochemistry* **2003**, *42*, 2806.
- (8) Each metal ion is ligated by two His in *Moorella thermoacetica* and *Thermotoga maritima* FDPs: Silaghi-Dumitrescu, R.; Kurtz, D. M., Jr.; Ljungdahl, L. G.; Lanzilotta, W. N. *Biochemistry* **2005**, *44*, 6492. In contrast, one of the two metal ions in *Desulfovibrio gigas* FDP is ligated by one His residue only: Frazao, C.; Silva, G.; Gomes, C. M.; Matias, P.; Coelho, R.; Sieker, L.; Macedo, S.; Liu, M. Y.; Oliveira, S.; Teixeira, M.; Xavier, A. V.; Rodrigues-Pousada, C.; Carrondo, M. A.; Le Gall, J. *Nat. Struct. Biol.* **2000**, *7*, 1041.
- (9) Hayashi, T.; Caranto, J. D.; Matsumura, H.; Kurtz, D. M., Jr.; Moënnelocoz, P. *J. Am. Chem. Soc.* **2012**, *134*, 6878.
- (10) Hayashi, T.; Caranto, J. D.; Wampler, D. A.; Kurtz, D. M., Jr.; Moënnelocoz, P. *Biochemistry* **2010**, *49*, 7040.
- (11) Feig, A. L.; Bautista, M. T.; Lippard, S. J. *Inorg. Chem.* **1996**, *35*, 6892.
- (12) Majumdar, A.; Lippard, S. J. *Inorg. Chem.* **2013**, *52*, 13292.
- (13) Zheng, S.; Berto, T. C.; Dahl, E. W.; Hoffman, M. B.; Speelman, A. L.; Lehnert, N. *J. Am. Chem. Soc.* **2013**, *135*, 4902.
- (14) Brown, C. A.; Pavlosky, M. A.; Westre, T. E.; Zhang, Y.; Hedman, B.; Hodgson, K. O.; Solomon, E. I. *J. Am. Chem. Soc.* **1995**, *117*, 715.
- (15) Lu, S.; Libby, E.; Saleh, L.; Xing, G.; Bollinger, J. M., Jr.; Moënnelocoz, P. *J. Biol. Inorg. Chem.* **2004**, *9*, 818.
- (16) Matsumura, H.; Hayashi, T.; Chakraborty, S.; Lu, Y.; Moënnelocoz, P. *J. Am. Chem. Soc.* **2014**, *136*, 2420.
- (17) McQuilken, A. C.; Ha, Y.; Sutherlin, K. D.; Siegler, M. A.; Hodgson, K. O.; Hedman, B.; Solomon, E. I.; Jameson, G. N.; Goldberg, D. P. *J. Am. Chem. Soc.* **2013**, *135*, 14024.
- (18) Blomberg, L. M.; Blomberg, M. R.; Siegbahn, P. E. *J. Biol. Inorg. Chem.* **2007**, *12*, 79.
- (19) The FTIR data do not distinguish whether visible illumination of 1a dissociates both nitrosyl ligands to produce a dynamic population of dinitrosyl and diferrous states or whether mononitrosyl species are produced after dissociation of only one NO molecule.
- (20) Caranto, J. D.; Weitz, A.; Hendrich, M. P.; Kurtz, D. M., Jr. *J. Am. Chem. Soc.* **2014**, *136*, 7981.
- (21) Do, L. H.; Hayashi, T.; Moënnelocoz, P.; Lippard, S. J. *J. Am. Chem. Soc.* **2010**, *132*, 1273.